EXCITONIC LUMINESCENCE IN SPHERICAL CORE-MULTI-SHELL QUANTUM DOT STRUCTURES

A Thesis Submitted to
the Graduate School of Engineering and Sciences of
İzmir Institute of Technology
in Partial Fulfillment of the Requirements for the Degree of

MASTER OF SCIENCE

in Physics

by
Cihan BACAKSIZ

July 2011
İZMİR

We approve the thesis of **Cihan BACAKSIZ**

Assoc. Prof. Dr. Ramazan Tuğrul SENGER
Supervisor

Prof. Dr. Nejat BULUT
Committee Member

Prof. Dr. İsmail SÖKMEN
Committee Member

07.07.2011

Prof. Dr. Nejat BULUT
Head of the Department of
Physics

Prof. Dr. Durmuş Ali DEMİR
Dean of the Graduate School of
Engineering and Sciences

ACKNOWLEDGMENTS

While I was studying about my thesis, there are some people around me who help and support me and hence deserve my special thanks.

Firstly, I would like to express my endless respect and gratitude to my supervisor Assoc. Prof. Dr. Ramazan Tuğrul SENGER. During my thesis work, he always made feel that he had confidence in me and supported me all the time. I am deeply grateful to him for these and also his very good guidance and encouraging. I think that studying with him is a milestone for me. I thank very much to give me the chance to study with him.

Besides my supervisor, I would like to thank to the members of my thesis defense committee Prof. Dr. Nejat BULUT and Prof. Dr. İsmail SÖKMEN for their contribution and giving suggestions.

I thank all my friends at Izmir Institute of Technology (IYTE) for their warm friendship and enjoyable times we spent. Especially, Ozan Arı, Onur Tosun, Oktay Doğangün and Mehmet Yağmurcukardeş who always take my side by helping, talking and spending our times with all together. They deserve my thanks for their support durring the study.

I would like to thank my family for their endless support and patience inspite of my studies and also their love.

ABSTRACT

EXCITONIC LUMINESCENCE IN SPHERICAL CORE-MULTI-SHELL QUANTUM DOT STRUCTURES

In this thesis, we studied excitonic light emission from core-multishell semiconductor hetero-nanocrystals having a spherically symmetric shape as a function of core size and shell thicknesses. Different combinations of semiconductors were considered in the core/shell/shell structure. The multilayer quantum dot structures that we considered were in A/B/A/B form, where A and B denote II-VI binary semiconductor crystals. We used method of finite differences to solve the Schrödinger equation of the confined exciton problem numerically. Several approximations including the effective mass approximation for the electron and hole masses, and treatment of Coulomb interaction as a perturbation, were employed. Normalized oscillator strengths for optical transitions and coexistence of multiple transitions from a single structure at several frequencies have been investigated. In this study, three different pairs of semiconductors are considered. One of them is (CdSe) ZnS) CdSe) ZnSe), other is (CdSe) CdS) CdSe) CdSe) and third one is (CdTe) ZnS) CdTe) ZnSe). According to our calculation, (CdSe)ZnS)CdSe)ZnSe) structure, when the core radius is 1.51 nm with some different shells combinations, has multi-color emissions from higher frequency to lower frequency in the visible spectrum. (CdSe) CdS) CdSe) CdSe) structure has multi-color emissions when the core radii are 2.02 nm and 2.52 nm yet this structure is the most inefficient structures which we analyse. Moreover, multi-color emissions are obtained from the structure (CdTe) ZnS) CdTe) ZnS) when the core radii are 1.29 nm, 1.93 nm, 2.58 nm and 3.23 nm. Also, this structure has nearly white light emission for 3.23 nm core radius with 3 ML ZnS shell and 1 ML CdTe shell, and with 4 ML ZnS shell and 1 ML CdTe shell.

ÖZET

ÇEKİRDEK-ÇOK KABUKLU KÜRESEL KUANTUM-NOKTA YAPILARIN EKSİTONİK IŞINIMI

Bu tezde, küresel simetriye sahip çekirdek çok kabuklu yarı iletken kuantum noktaların çekirdek büyüklüğüne ve kabuk kalınlıklarına bağlı olarak görünür dalga boyundaki ışınımları üzerine çalışıldı. Farklı yarı iletken çiftlerinin çekirdek/kabuk/kabuk biçiminde sırayla katmanlandığı farz edildi. Hapsedilmiş eksitonun Schrödinger denklemini nümerik olarak çözmek için sonlu eleman yöntemi kullanıldı. Hesaplamalarımız yapılırken, etkin kütle yaklaşımı ve Coulomb etkileşimini pertürbasyon olarak almak gibi çeşitli yaklaşımlar kullanıldı. Ayrıca, optik geçişler hakkında fikir edinilmesi için, üzerinde çalıştığımız kuantum noktalarda oluşan her bir eksitona ait normalize edilmiş salınım güçleri hesaplandı. Bu çalışmada, üç farklı yarıiletken çiftinden oluşmuş yapılar incelendi. Bunlardan biri CdSe) ZnS) CdSe) ZnSe), bir diğeri (CdSe) CdS) CdSe) CdSe) ve üçüncüsü ise (CdTe) ZnS) CdTe) ZnSe). Hesaplarımıza göre, 1.51 nm'lik çekirdek yarıçapına sahip (CdSe) ZnS) CdSe) ZnSe) yapısı, bazı kabuk kombinasyonlarında, yüksek frekanslaradan düşük frekanslara, çok renkli ışıma yapıyor. (CdSe) CdS) CdSe) CdSe) yapısı ise, 2.02 nm ve 2.52 nm'lik çekirdeği olduğu durumlarda, çok renkli ışıma yapıyor fakat incelenen yapılar arasında en verimsiz olanı (CdSe) CdS) CdSe) CdSe) yapısı. Bunlara ek olarak, (CdTe) ZnS) CdTe) ZnS) yapısı 1.29 nm, 1.93 nm, 2.58 nm ve 3.23 nm'lik çekirdeği olduğu hallerde çok renkli ışımaya sahip. Ayrıca, (CdTe) ZnS) CdTe) ZnS) yapısı, 3.23 nm çekirdek 3 ML'lık ZnS kabuğu ve 1 ML'lık CdTe kabuğuyla ve de 4 ML'lık ZnS kabuğu ve 1 ML'lık CdTe kabuğuyla, beyaz ışık ışımasına yakın bir ışıma yapmaktadır.

TABLE OF CONTENTS

LIST OF FIGURES

Figure **Page**

LIST OF TABLES

CHAPTER 1

INTRODUCTION

Nowadays the requiring faster and smaller devices forced to natural limits in microelectronics, for this reason, different approaches and studies are needed to achieve practical low dimensional systems. During the past years concern about nano scale systems highly increased therefore synthesis of functional nano-materials exhibited considerable developments with their controllable size, shape, electronic and optical properties.

One of these focused issues are nano-dimensional semiconductor structures at which quantum-size effects start to dominate as electron and hole motions are confined attwo particle reach to two particle reach to two particle reach to least one dimensions. In bulk semiconductors, electron at the valance band is excited by absorbed photon. The required energy for excitation is is indicated by energy band gap of semiconductor. The excited electron leaves behind positive charged particle (hole) at the valance band. Electron at the conduction band and hole at the valance band are attracted to each other by Coulomb force. Bound state of these electron and hole is named exciton. When an exciton recombine means electron back to valance band, it emits photon so the excitonic luminescence occurs. In quantum dot, energy levels in valance and conduction bands have discrete distribution and the band gap is larger than compared to bulk state because of Quantum confinement effects. Quantum confinement effects occur when the size of structure is comparable to Bohr radius of electron-hole pair (exciton). Bohr radius is smallest possible orbit radius which is about 10 nm for electron hole pair in semiconductors. Therefore, when the size of semiconductor crystal is comparable to 10 nm, excitonic luminescence has quantized energy levels and is possible to occur in visible spectrum.

The quantum confinement effects was first observed in the 1920's that when the absorption and luminescence of heated glasses containing CdS colloids color shifts to smaller wavelengths. In the 1960's, it was reported that there were differences between absorption spectra of colloidal semiconductor particles and spectra of the corresponding bulk materials [3–5]. Soon after the invention of Molecular Beam Epitaxy (MBE) [6, 7], quantized energy levels of confined charge carriers in 2D-structures were confirmed by experimental observation [8]. Afterward, this intresting effects were attracted considerable attention by theoretical and experimental studies [9–22]. Theoretical studies were started in the 1980's for the effect of size on electronic structures. The first theoretical de-

scriptions about the nature of the 3D excitonic quantum confinement were given by Efros and Efros [10] and by Brus [9]. Progressive different theoretical studies and improvement in synthesis techniques allowed various works on nano-crystals [23–31]. These works were also extended to complex nano-structures like coated semiconductor particles which included layers of shells with different semiconductors surrounding core of quantum dot, so called core/shell quantum dot. The first effort on core/shell quantum dot was obtained by using HgS layer on CdS core and CdS layer on them in 1993 [31]. Then, (CdS)CdSe/CdS and (ZnS)CdS/ZnS structures were successfully synthesized, and some of then also theoretically investigated [32–36] These early core/shell or core/shell/shell quantum dots had light emissions in only mono color. But the there is a strong demand for multi-color emitting nanocrystal systems. To obtain different color or white light, different types of nanocrystals must be carefully combined. In stead of that, multi-color or white light emitting systems using only a single type of nanocrystal are more convenient for fabrication and for efficient emission.

On the other hand, quantum dots with specified properties are put to use on so many areas and on stand by many others.

First of all, today fluorescent quantum dots are successfully used for diagnostics in biology. Nanocrystal particles have tunable and distinct spectrum of emission and long life compared to conventional fluorophores. Semiconductor quantum dots are easily bound to proteins and DNA molecules so that biological reactions can be followed. Because of these properties, semiconductors quantum dots have promising future for further imaging techniques for the biological processes.

Another potential applications are opto-electronics devices such as light emitting diodes (LEDs), photovoltaic cells and lasers. Combination of optical and electronic properties of semiconductors quantum dots and white light emitting systems are the real achievements. In recent years, considerable progress has been made in this route [37, 38].

In this thesis, multi-color light emission from core-multishell semiconductor quantum dots are treated. In the next chapter, the theoretical bases on which our numerical study is standing are given, then numerical representations are shown. Results of our computations are discussed last two chapters.

CHAPTER 2

METHOD

2.1. Theory

First of all, to solve our problem of electron-hole pair in spherical symmetric quantum dot heteronanocrystal structure, it is necessary to give general Hamiltonian,

$$H = -\frac{\hbar^2}{2m_e}\overrightarrow{\nabla}_e^2 - \frac{\hbar^2}{2m_h}\overrightarrow{\nabla}_h^2 - \frac{1}{4\pi\varepsilon}\frac{e^2}{|\mathbf{r}_e - \mathbf{r}_h|} + V_e(\mathbf{r}_e) + V_h(\mathbf{r}_h) + E_g. \qquad (2.1)$$

Here ε is the dielectric constant of semiconductor material. E_g is the band gap energy of bulk semiconductor material. $\mathbf{r}_e$, m_e, $V_e(\mathbf{r}_e)$ and $\mathbf{r}_h$, m_h, $V_h(\mathbf{r}_h)$ are position, the effective mass, potential well height of electron and hole, respectively.

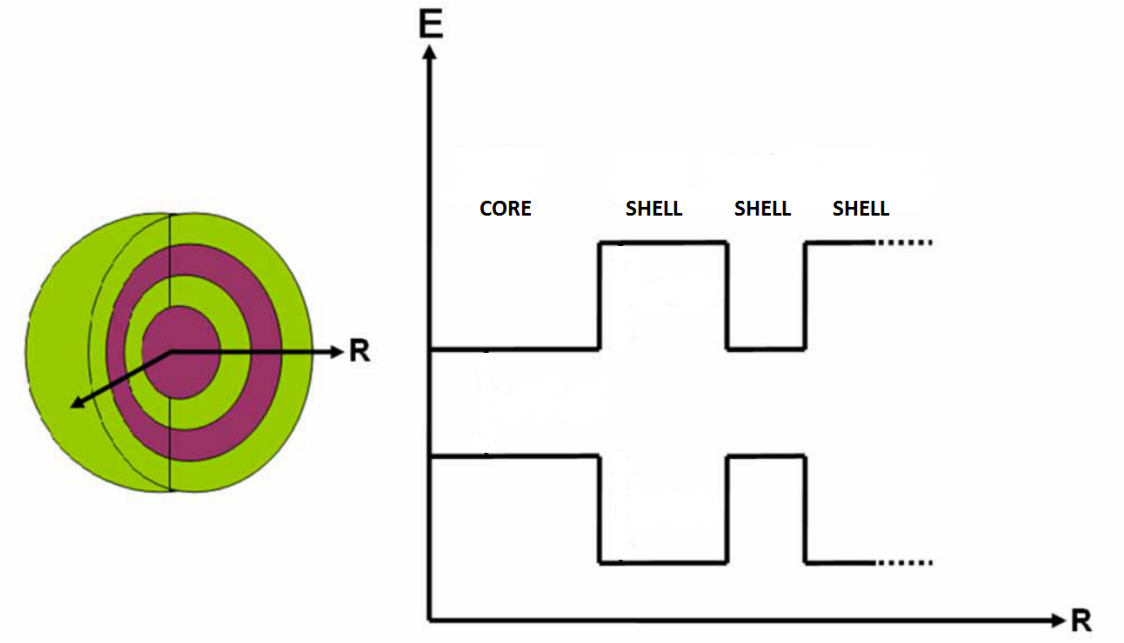

Figure 2.1. Left: Schematic of core-multishell semiconductor hetero-nanocrystal. Right: Radial energy diagram (not drawn to scale)[1]

The theoretical analysis starts with assuming strong confinement potential so that the Coulomb interaction between electron and hole is negligible comparatively. Also because

of the mass of electron and hole may depend on the position, we applied effective mass approximation which works well even for nano-dimensional structure [27, 39–43].

2.1.1. One Particle States

For single electron or hole, Schrödinger equation, without considering Coulomb interaction, can be written in the form of

$$\left[-\frac{\hbar^2}{2}\overrightarrow{\bigtriangledown}\frac{1}{m(\mathbf{r})}\overrightarrow{\bigtriangledown}+V(\mathbf{r})\right]\psi(\mathbf{r})=E\psi(\mathbf{r}), \tag{2.2}$$

$$\psi_{nlm}(r,\theta,\phi)=R_{nl}(r)Y_{lm}(\theta,\phi). \tag{2.3}$$

We consider a sphericaly symmetric heteronanocrystal structure, in order to separate the angular and the radial part of the equation. In Equation (2.2), $\psi_{nlm}(r,\theta,\phi)$ represents the wavefunction of the corresponding particle in spherical coordinates (r,θ,ϕ), $R_{nl}(r)$ is radial wavefunction, $Y_{lm}(\theta,\phi)$ is the spherical harmonics, n is the principal quantum number, m and l are the angular momentum quantum numbers.

$$V(r)=\begin{cases} V_1 & for \quad 0\leq r<r_1 \\ V_2 & for \quad r_1\leq r<r_2 \\ \vdots & \\ V_N & for \quad r_{N-1}\leq r<r_N \end{cases} \tag{2.4}$$

The confinement potential written in Equation (2.3) is assumed stepwise constant value throughout distinct regions. At all regions, confinement potentials are spherically symmetric that means there is no angular dependence but there is only radial dependence. In the spherical symmetric case, $m=0$ and $l=0$, angular part of the wavefunction gives

constant factor of $1/\sqrt{4\pi}$ and radial eigenfunction $R_{nl}(r)$ in the N regions is stated,

$$R_{nl}(r) = \begin{cases} R_{nl,1} & for \quad 0 \leq r < r_1 \\ R_{nl,2} & for \quad r_1 \leq r < r_2 \\ \quad \vdots & \\ R_{nl,N} & for \quad r_{N-1} \leq r < r_N \end{cases} \tag{2.5}$$

Two case is distinguished to find $R_{nl}(r)$; in regions where $E_{nl} > V_q$, the solution is a linear combination of spherical Bessel and Neumann functions as

$$R_{nl,q}(r) = A_{nl,q} j_l(k_{nl,q} r) + B_{nl,q} n_l(k_{nl,q} r), \tag{2.6}$$

with

$$k_{nl,q} = \sqrt{\frac{2m_q(E_{nl} - V_q)}{\hbar^2}}, \tag{2.7}$$

on the other hand, in the case of $E_{nl} < V_q(q$, the wave equation yields linear combination of Hankel functions $h_l^{(+)}$ and $h_l^{(-)}$ as

$$R_{nl,q}(r) = A_{nl,q} h_l^{(+)}(\kappa_{nl,q} r) + B_{nl,q} h_l^{(-)}(\kappa_{nl,q} r), \tag{2.8}$$

with

$$\kappa_{nl,q} = \sqrt{\frac{2m_q(V_q - E_{nl})}{\hbar^2}}, \tag{2.9}$$

At the crossing of regions, the general solution must satisfy the boundary conditions [44, 45],

$$R_{nl,q}(r_q) = R_{nl,q+1}(r_q) \tag{2.10}$$

$$\frac{1}{m_q}\frac{dR_{nl,q}(r)}{dr}\Big|_{r=r_q} = \frac{1}{m_{q+1}}\frac{dR_{nl,q+1}(r)}{dr}\Big|_{r=r_q} \tag{2.11}$$

After applying the requirements, $R_{nl}(r)$ has to be regular at $r = 0$ and has to converge to zero when $r \to \infty$. N regions means $N - 1$ boundaries, Equation (2.9) and (2.10) leads to $2N - 2$ equalities and $2N - 2$ unknown coefficients $A_{nl,q}$, $B_{nl,q}$. To find the nontrivial solution of this linear equation system, the determinant of unknown coefficients have to be zero,

$$D_l = D_l(E_{nl}) = 0. \tag{2.12}$$

After finding the eigenvalue as a single zero of Equation (2.11), the linear equations can be solved as a function of $A_{nl,q}$ or $B_{nl,q}$ and last unknown coefficient is determined by the normalization of $R_{nl}(r)$ [31, 40]. These calculations gives the wave function of single electron or single hole and corresponding energy of its state with no interaction.

2.1.2. The Coulomb Interaction

At the beginning of analysis, our first assumption is strong confinement potential therefore, by using the first order perturbation theory, the exciton binding energy due to Coulomb interaction between electron and hole is written as [31];

$$E_c = -\frac{e^2}{4\pi}\iint d\mathbf{r}_e d\mathbf{r}_h \frac{\psi_e^*(\mathbf{r}_e)\psi_h^*(\mathbf{r}_h)\psi_e(\mathbf{r}_e)\psi_h(\mathbf{r}_h)}{|\mathbf{r}_e - \mathbf{r}_h|}\frac{1}{\bar{\varepsilon}(\mathbf{r}_e, \mathbf{r}_h)} \tag{2.13}$$

In Equation (2.12), e and h represent electron and hole, and ε is effective dielectric constant. $1/|\mathbf{r}_e - \mathbf{r}_h|$ is expended in the form of spherical harmonics by using cosines law with angle θ_h which is the angle between $\mathbf{r}_e$ and $\mathbf{r}_h$ when $\mathbf{r}_e$ is fixed on polar axis.

$$|\mathbf{r}_e - \mathbf{r}_h| = \sqrt{r_e^2 + r_h^2 - 2r_e r_h \cos\theta_h}. \tag{2.14}$$

For the effective dielectric constant $\bar{\varepsilon}(r_e, r_h)$ in Equation (2.12), we make an approximation over volume of shells considering the boundary values to calculate mean dielectric

constant because materials have different dielectric constant. If the fractions of distance between electron and hole in different material is regarded, the calculation of effective dielectric constant so all calculation become exceedingly heavy.

$$\bar{\varepsilon}(r_e, r_h) = \begin{cases} \varepsilon_1 & for \quad r_{max} < r_1 \\ \varepsilon_{r_{max}} & for \quad r_1 < r_{max} < r_2 \\ \frac{\varepsilon_3(r_{max}^3 - r_2^3) + \varepsilon_2(r_2^3 - r_1^3) + \varepsilon_3 r_1^3}{r_{max}^3} & for \quad r_2 < r_{max} < r_3 \end{cases} \tag{2.15}$$

In Equation (2.14), r_1, r_2, r_3 are radius of core and shell boundaries, ε_1, ε_2, ε_3 are dielectric constant at core, first shell and second shell, respectively. r_{max} refers to larger of r_e and r_h. $\varepsilon_{r_{max}}$ is the dielectric constant at the position where larger of r_e and r_h refers. Hereby, effective dielectric constant becomes free from angular dependence. After separating the variables of wave functions and conjugate wave functions in spherical coordinates, the Coulomb energy is expressed as

$$\begin{aligned} E_c = -\frac{e^2}{4\pi} \int_0^{2\pi} \int_0^{\pi} d\theta_e d\phi_e \sin\theta_e |Y_e(\theta_e, \phi_e)|^2 \int_0^{2\pi} d\phi_h |Y_h(\theta_h, \phi_h)|^2 \\ \times \iint dr_e dr_h r_e^2 r_h^2 \int_0^{\pi} d\theta_h \sin\theta_h \frac{|R_e(r_e)|^2 |R_h(r_h)|^2}{\sqrt{r_e^2 + r_h^2 - 2r_e r_h \cos\theta_h}} \frac{1}{\bar{\varepsilon}(r_e, r_h)} \end{aligned} \tag{2.16}$$

Here, $\psi_e(\mathbf{r}_e) = R_e(r_e)Y_e(\theta_e, \phi_e)$ and $\psi_h(\mathbf{r}_h) = R_h(r_h)Y_h(\theta_h, \phi_h)$.

$$\begin{aligned} E_c = -\frac{e^2}{4\pi} \int_0^{2\pi} \int_0^{\pi} d\theta_e d\phi_e \sin\theta_e |Y_e(\theta_e, \phi_e)|^2 \int_0^{2\pi} d\phi_h |Y_h(\theta_h, \phi_h)|^2 \\ \times \iint dr_e dr_h r_e^2 r_h^2 |R_e(r_e)|^2 |R_h(r_h)|^2 \frac{1}{\bar{\varepsilon}(r_e, r_h)} \left(\frac{\sqrt{r_e^2 + r_h^2 - 2r_e r_h \cos\theta_h}}{r_e r_h} \Big|_0^{\pi} \right) \end{aligned} \tag{2.17}$$

$l = m = 0$ because of spherical symmetry, and the angular part of the wavefunction is constant value, $Y_{e,lm}(\theta_e, \phi_e) = Y_{h,lm}(\theta_h, \phi_h) = 1/\sqrt{4\pi}$.

$$E_c = -\frac{e^2}{4\pi} \int_0^{2\pi} \int_0^{\pi} d\theta_e d\phi_e \sin\theta_e |Y_e(\theta_e, \phi_e)|^2 \int_0^{2\pi} d\phi_h |Y_h(\theta_h, \phi_h)|^2 \times \iint dr_e dr_h r_e^2 r_h^2 \frac{|R_e(r_e)|^2 |R_h(r_h)|^2}{\bar{\varepsilon}(r_e, r_h)} \frac{1}{r_e r_h} \left[(r_e + r_h) - |r_e - r_h|\right] \tag{2.18}$$

After integration over the angular coordinates, the equation becomes;

$$E_c = -\frac{e^2}{4\pi\varepsilon_0} \int_0^{\infty} dr_e \left[\int_0^{r_e} dr_h r_e r_h^2 |R_e(r_e)|^2 |R_h(r_h)|^2 \frac{1}{\bar{\varepsilon}(r_e, r_h)} + \int_{r_e}^{\infty} dr_e r_e^2 r_h |R_e(r_e)|^2 |R_h(r_h)|^2 \frac{1}{\bar{\varepsilon}(r_e, r_h)} \right] \tag{2.19}$$

For the simpler representation,

$$E_c = -\frac{e^2}{4\pi\varepsilon_0} \iint dr_e dr_h r_e^2 r_h^2 \frac{|R_e(r_e)|^2 |R_h(r_h)|^2}{max(r_e, r_h)} \frac{1}{\bar{\varepsilon}(r_e, r_h)}. \tag{2.20}$$

After determining the Coulomb energy, the transition energy can be written as,

$$E_{tr} = E_e + E_h + E_c + E_{sm}, \tag{2.21}$$

E_e and E_h are single particles eigen energy without interaction between them, E_c is Coulomb energy and E_{sm} is smallest band gap energy of materials that are used in structure. Transition energy is recombination energy of exciton so the energy of emitted light.

2.1.3. Oscillator Strength

In our analysis, oscillator strength of the excitons are also calculated. Oscillator strength is dimensionless quantity which expresses the transition ability of an exciton from one quantum state to another. This transition is the source of light from quantum dot, thus oscillator strength gives the idea about dominant color of emitted light. Simply, calculation overlapping of single electron and hole wavefunction and dividing by binding energy of corresponding energy gives the recombination probability [46]. The envelope function of exciton is;

$$\Psi_{ex}(\mathbf{r}) = \psi_e(\mathbf{r}_e)\psi_h(\mathbf{r}_h)\phi(|\mathbf{r}_e - \mathbf{r}_h|), \tag{2.22}$$

and the oscillator strength is written as;

$$f_{ex} \propto \frac{1}{E_c}\left[\int \Psi_{ex}(\mathbf{r} = \mathbf{r}_e = \mathbf{r}_h)d\mathbf{r}\right]^2, \tag{2.23}$$

where E_c is the Coulomb interaction between electron and hole. Not the exact value of oscillator strength, we are interested in comparison of oscillator strengths values of states in related quantum dot.

2.2. Numerical Approach

2.2.1. Finite Difference Method

The finite difference method is a basic numerical method which is based on the approximation of derivatives of the function with respect to grids on the variable of the function and equal differences between these grids. Let f be the function of variable r which has finite steps of h (h refers to hole when it is used as subscript otherwise it is step size) stated in Equation (2.24) and (2.25),

$$r_i = r_0 + ih \qquad (i = 1, 2, 3, ...)\ , \tag{2.24}$$

$$h = r_{i+1} - r_i \ . \tag{2.25}$$

Taylor expansion of f around r_i is;

$$f(r_i + h) = f(r_i) + hf^{'}(r_i) + \frac{h^2}{2!}f^{''}(r_i) + \frac{h^3}{3!}f^{'''}(r_i) + ... \tag{2.26}$$

Thus first derivative of f at point r_i is approximately written as

$$f^{'}(r_i) \approx \frac{f(r_i + h) - f(r_i)}{h}, \tag{2.27}$$

Equation (2.27) is the forward difference derivative formula. Taylor expansion of $f(r_i - h)$ and first derivative which is named as backward difference derivative formula;

$$f(r_i - h) = f(r_i) - hf^{'}(r_i) + \frac{h^2}{2!}f^{''}(r_i) - \frac{h^3}{3!}f^{'''}(r_i) + ... \tag{2.28}$$

$$f^{'}(r_i) \approx \frac{f(r_i) - f(r_i - h)}{h}, \tag{2.29}$$

Forward difference and backward difference derivative formulas have error order of h. There is more consistent formula for first derivative. Subtracting Equation (2.28) from (2.26) gives first derivative formula as;

$$f^{'}(r_i) \approx \frac{f(r_i + h) - f(r_i - h)}{2h} \tag{2.30}$$

This is named central deference derivative derivative formula which has error order of h^2. Similarly sum of Equation (2.28) and (2.26) yields second derivative formula as;

$$f^{''}(r_i) \approx \frac{f(r_i + h) - f(r_i - h) - 2f(r_i)}{h^2} \tag{2.31}$$

Now Schrödinger equation for the single particle can be written by substituting the derivative formula.

2.2.2. Schrödinger Equation Numerical Form

In order to write the Schrödinger equation of our system in useful form for numerical calculation, simple operations such as reducing the equation in dimensionless form and applying the approximate derivative formula are applied. The eigen energies and the eigen functions of a single particle in the structure are determined by calculation of computer program after numerical form is coded.

Firstly, separated variables of (r, θ, ϕ) and the spherical symmetry on the system gives the radial wave equation of single particle in the form of;

$$\frac{d}{dr}\left(r^2 \frac{dR}{dr}\right) - \frac{2mr^2}{\hbar^2}\left[V(r) + E\right] R = l(l+1)R. \tag{2.32}$$

To simplify the Equation (2.32), variables are changed,

$$U(r) \equiv rR(r), \tag{2.33}$$

Radial equation transforms to one dimensional Schrödinger equation,

$$EU = \frac{\hbar^2}{2}\left[\frac{d}{dr}\left(\frac{1}{m(r)}\frac{d}{dr}U\right)\right] + \left[V + \frac{\hbar^2}{2m(r)}\frac{l(l+1)}{r^2}\right]U. \tag{2.34}$$

To write in numerical form, derivative formula defined by finite difference approximation, which is adverted before, is applied to Equation (2.34),

$$EU_i = \frac{\hbar^2}{2}\left[\frac{\left(\frac{1}{m_{i+1}} - \frac{1}{m_{i-1}}\right)}{2h}\frac{(U_{i+1} - U_{i-1})}{2h} + \frac{1}{m_i}\frac{(U_{i+1} - U_{i-1} - 2U_i)}{h^2}\right] + \left[V + \frac{\hbar^2}{2m_i}\frac{l(l+1)}{r_i^2}\right]U_i \tag{2.35}$$

In the equation, h refers size of steps. i is indice which counts the h on the position axis from zero to end of considered length say it is the radius of quantum dot. U_i represents numerical value at the i'th step from zero. The equation needs derivation to be more convenient for computer programming. First of all, it has to be written in dimensionless form.

$$EU_i = \frac{\hbar^2}{2h^2}\left[\left(\frac{1}{4m_{i+1}} - \frac{1}{4m_{i-1}}\right)(U_{i+1} - U_{i-1}) + \frac{1}{m_i}(U_{i+1} - U_{i-1} - 2U_i)\right] \tag{2.36}$$
$$+ \left[V + \frac{\hbar^2}{2m_i}\frac{l(l+1)}{r_i^2}\right]U_i$$

To construct a factor in the unit of energy, the right side of the equation is multiplied and divided with m_e. Angular momentum quantum number, $\frac{\hbar^2}{2m_i}\frac{l(l+1)}{r_i^2}$ is zero.

$$l = 0, \tag{2.37}$$

thus

$$\frac{\hbar^2}{2m_i}\frac{l(l+1)}{r_i^2} = 0, \tag{2.38}$$

the equation takes a form as

$$EU_i = \frac{\hbar^2}{2h^2 m_e}\left[\left(\frac{m_e}{4m_{i+1}} - \frac{m_e}{4m_{i-1}} + \frac{m_e}{m_i}\right)U_{i+1} + \left(-\frac{m_e}{4m_{i+1}} + \frac{m_e}{4m_{i-1}} + \frac{m_e}{m_i}\right)U_{i-1}\right] \tag{2.39}$$
$$+ \left[-\frac{\hbar^2}{2h^2 m_e}\frac{2m_e}{m_i} + V\right]U_i.$$

If we say

$$\frac{\hbar^2}{2h^2 m_e} \equiv \boldsymbol{\epsilon}, \tag{2.40}$$

and divide both sides with ϵ and edit the equation, then the dimensionless eigenvalue equation is constructed as

$$\frac{E}{\epsilon}U_i = \left(\frac{m_e}{4m_{i+1}} - \frac{m_e}{4m_{i-1}} + \frac{m_e}{m_i}\right)U_{i+1} + \left(\frac{V}{\epsilon} - \frac{2m_e}{m_i}\right)U_i + \left(-\frac{m_e}{4m_{i+1}} + \frac{m_e}{4m_{i-1}} + \frac{m_e}{m_i}\right)U_{i-1} \tag{2.41}$$

This form of equation is ready to compute as $N \times N$ tridiagonal matrix where N is the considered number of steps on the radius of quantum dot. The matrix is specified with entering the core and shell sizes, band gap energies, effective mass of electron and hole, and dielectric constants with respect to indice that counts the steps on the radius.

2.2.3. The Coulomb Interaction in Numerical Form

After determining the eigen states, we write down the effective dielectric constant and the Coulomb interaction in proper form for numerical computation as

$$\bar{\varepsilon}(r_a, r_b) = \begin{cases} \varepsilon_1 & for \quad r_{max} < r_1 \\ \varepsilon_{r_{max}} & for \quad r_1 < r_{max} < r_2 \\ \frac{\varepsilon_3(r_{max}^3 - r_2^3) + \varepsilon_2(r_2^3 - r_1^3) + \varepsilon_3 r_1^3}{r_{max}^3} & for \quad r_2 < r_{max} < r_3 \end{cases} \tag{2.42}$$

Here, a, b and c is the dummy indices from zero to N for electron and hole, respectively. $r_a = ah$, $r_b = bh$ and $r_c = ch$ (h refers to hole when it is used as subscript otherwise it is step size), max is present the larger of r_e and r_h. r_1, r_2, r_3 are radius of core and shell boundaries. ε_1, ε_2, ε_3 are dielectric constant at core, first shell and second shell, respectively.

$$E_c = -\frac{e^2}{4\pi\varepsilon_0}\sum_{a=1}^{N}\left[\sum_{b=1}^{a} h^2(ah)(bh)^2|R_e(a)|^2|R_h(b)|^2\frac{1}{\bar{\varepsilon}(r_a, r_b)} + \sum_{c=a}^{N} h^2(ch)^2(bh)|R_e(c)|^2|R_h(b)|^2\frac{1}{\bar{\varepsilon}(r_a, r_b)}\right] \tag{2.43}$$

In Eqn.(2.44), h is the step size and a is the integer number so ah refers a length as bh does. If N is sufficiently high means h is small, the calculation is more accurate.

2.2.4. Oscillator Strength in Numerical Form

Another required value that we represented before is oscillator strength after computing the Coulomb interaction. The summation which is used for Coulomb interaction is also convenient for calculation the oscillator strength. Angular parts of the wave functions of electron and hole give constant value so we do not consider.After that, integration over radial part of the envelope function is formed as,

$$f_{ex} = \frac{1}{E_c}\left[\sum_{a=b=1}^{N}(ah)(bh)R_e(a)R_h(b)h\right]^2, \tag{2.44}$$

a, b are dummy indices again, h is step size(h refers to hole when it is used as subscript), $R_e(r_a)$ is the value of electron radial wavefunction at the position of ah and $R_h(r_b)$ is the value of hole radial wavefunction at the position of bh.

CHAPTER 3

RESULTS

Before giving the results, we would like to provide some information on the stages of calculation. In our analysis, we take two types of semiconductors spherically layered in the form of (core) shell) shell) shell). Core and the second shell are of the same material whereas the first shell and the last shells are of the other semiconductor. Firstly, a spherical core is considered with a radius of n mono-layer thickness, then another material is layered on the core as a shell with m mono-layer thickness, and then the core material is layered again on the first shell as second shell with a thickness of k mono-layers. Last shell covering the quantum dot is considered infinitely thick. In order to engineer the excitonic properties of the multi-layered quantum dots, the core radii are varied from 2 mono-layer to 5 mono-layer and shells thicknesses are varied from 1 mono-layer to 4 mono-layer ($n = 2..5, m = 1..4, k = 1..4$). First three eigenfunctions of single electron and single hole, Coulomb energies, transition energies between electron and hole for all three states which means nine couples and oscillator strength of these couples are computed for all combinations of core-shell sizes.

In our investigation, three different pairs of semiconductors are considered. One of them is (CdSe) ZnS) CdSe) ZnSe), other is(CdSe) CdS) CdSe) CdSe) and third one is (CdTe) ZnS) CdTe) ZnSe). One of the reasons to choose these pairs is the difference between their band gap energies. Electron and hole are expected to be localized in the regions of the quantum dot with the smaller band gap energy. Variations in electron and hole localization regions and variation in eigenenergies are desired so that result to have different transition energies and different colors of emitted light can be obtained. Also, presence of alternative localization regions for electron and hole is important for achieving multi-color emission from the same dot.

In Table 3.1, we list bulk energy band gap value, effective masses of the electron and hole, mono-layer thickness and dielectric constant of the bulk materials material that we considered.

In the tables of results section, some specific configurations which show multi-color emission are given. First three columns inform the core and shell sizes, column of (n_e, n_h) gives the states of single particles which form an exciton, transition energy column gives the emission energies from recombination of those excitons, and column

Table 3.1. Material Parameters[2]

Material	$\mathbf{E_g(eV)}$	$\mathbf{m_e^*/m_e}$	$\mathbf{m_h^*/m_e}$	**ML (nm)**	ε
ZnS	3.75	0.28	0.49	0.54 (czb)	8.31
CdS	2.48	0.21	0.64	0.486 (wrt)	5.26
CdTe	1.47	0.095	0.12,0.81	0.646 (zb)	7.1
CdSe	1.74	0.12	0.45	0.505 (wrt)	6.26

of oscillator strength gives the ratio of relatively high oscillator strengths for those core-shell-shell sizes. Also probability distributions of single electron and hole, which create exciton with a relatively high oscillator strength, are shown in corresponding figures.

3.1. CdSe-ZnS

One of the structures which we analyse is (CdSe) ZnS) CdSe) ZnSe). In Table 3.2, for 1.51 nm core radius, some significant multi-color emission cases. In Figure 3.1 and 3.2, it is shown that all the electrons are localized at the CdSe core and all the holes are localized at CdSe shell, in these cases. According to our calculation, (CdSe) ZnS) CdSe) ZnSe) structure with 1.51 nm core would emit various colors from higher frequency to lower frequency in the visible spectrum.

At first three rows of Table 3.2, structures have 3 ML ZnS shell(first shell) and at other three rows, structures have 4 ML ZnS shell. For both cases (with 3 and 4 ML ZnS shell), whatever the thickness of first shell is, the thickness of second shell determines the emission frequency. When structure have 3 ML ZnS shell with 1 ML CdSe shell has two different excitonic states which are created by electron and hole having single particle states of (1,2) and (2,2), and the case with 2 ML CdSe shell has the same excitonic states, but emission energies are different. But, when CdSe shell (second shell) thickness is with 1 ML, for both 3 ML and 4 ML ZnS shell, almost same transition energies are found. Also

Table 3.2. Some specific multi-color emission results for the structure (CdSe) ZnS) CdSe) ZnS) when core radius is **1.51** nm

Core Radius (nm)	**Shell Size (ML)**	**Shell Size (ML)**	**States ($\mathbf{n}_e, \mathbf{n}_h$)**	**Transition Energy (eV)**	**Oscillator Strength**
1.51	3	1	(1,2) (2,2)	3.06 2.07	6 5
1.51	3	2	(1,2) (2,2)	1.79 2.32	1 1
1.51	3	3	(2,1) (2,3)	2.65 3.16	4 3
1.51	4	1	(1,2) (2,2)	3.10 2.14	4 3
1.51	4	2	(1,2) (2,2)	1.72 2.55	1 1
1.51	4	3	(2,1) (2,3)	2.62 3.18	5 4

when the structure has 3 ML or 4 ML ZnS shell, they have almost same emission energies, if they have the same CdSe shell thickness. The reason of small increases in transition energies for structure with 4 ML ZnS shell is that 4 ML ZnS is a stronger barrier for an electron which is localized at core as shown in Figure 3.1 , so the confinement effect is stronger. Thus, the emission energies are determined by the thickness of CdSe shell (second shell) for the 3 ML and 4 ML ZnS shell cases.

3.2. CdSe-CdS

One of the other structures that we investigate is (CdSe)CdS)CdSe)CdSe). In Table 3.3, for core sizes 2.02 nm and 2.52 nm, it is given that some shell sizes have multi-color emission. According to our calculation, for smaller core sizes, only mono-color emission is observed. Mono-color emission energy is changing from red to yellow with very little increasing frequency when we are increasing the core size. On the other hand, when structure have 2.02 nm core size, two different shell combination give multi-color emission. One of them is with 2 ML CdS shell(first shell) and 4 ML CdSe shell(second shell), and 4 ML CdS shell and 4 ML CdSe shell. For both cases, one of excitonic emissions is from (2,2) electron and hole state, despite being at same states, excitons have different emission energies. In Figure 3.3, it is shown that electron and hole are localized at core, but for the case with 4 ML CdS shell, hole have larger penetration to second shell,

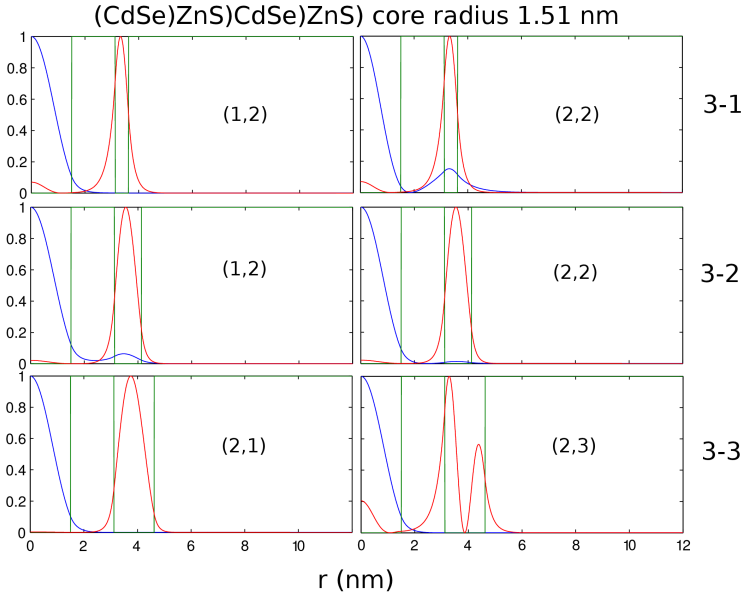

Figure 3.1. Relative probability distribution of electron (blue) $|R_e(r_e)|^2$, hole (red) $|R_h(r_h)|^2$ and potential(green) $V(r)$ of structure (CdSe) ZnS) CdSe) ZnS) with core radius 1.51 nm. In our notation, x-y means x mono-layer first shell and y mono-layer second shell (for example '3-1' indicates 3 mono-layer first shell and 1 mono-layer second shell). Also for (x,y) representation, x means n_e quantum number of electron and y means n_h quantum number of hole (for example (1,2) means electron is at ground state and hole is at first excited state). All peaks are normalized to 1.

which has larger volume to avoid confinement effect, therefore, The Coulomb energy is smaller because of difference in localization of electron and hole, and also 4 ML shell is stronger barrier and it makes the confinement effect is stronger for electron which is totaly localized in core. So increasing the emission energy for same states of electron and hole from 2 ML CdS shell to 4 ML CdS shell is reasonable. In addition to this, for 2.02 nm CdSe core with 2 ML CdS shell and 4 ML CdSe shell, the highest excitonic emission energy is from (2,2) electron and hole states which are localized totally in CdSe core.

On the other hand, in Figure 3.4, it is shown that all multi-color excitonic emissions are from core of the quantum dot for the case of 2.52 nm CdSe core. Also, in the Table 3.3, there are three different excitonic emissions from the structure of 4 ML CdS shell with 1 ML CdSe shell, but the frequencies are very close to each other.

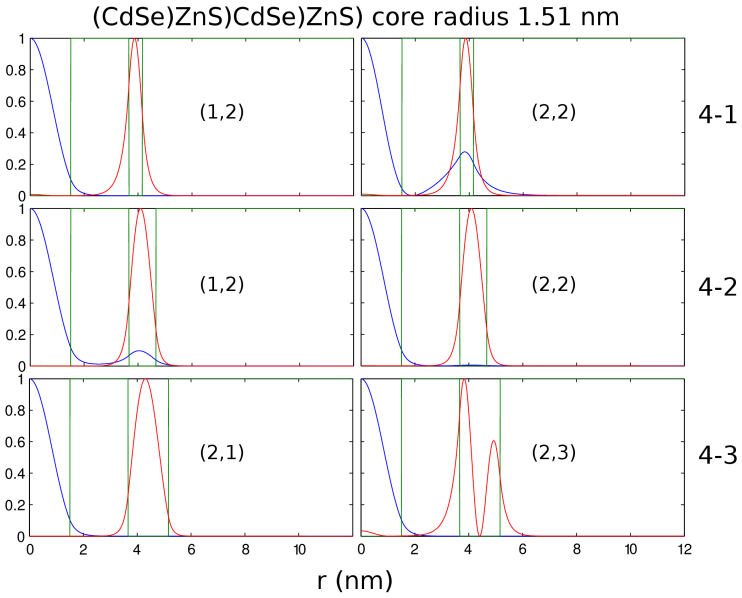

Figure 3.2. Relative probability distribution of electron (blue) $|R_e(r_e)|^2$, hole (red) $|R_h(r_h)|^2$ and potential(green) $V(r)$ of structure (CdSe) ZnS) CdSe) ZnS) with core radius 1.51 nm. In our notation, x-y means x monolayer first shell and y monolayer second shell (for example '4-1' indicates 4 monolayer first shell and 1 monolayer second shell). Also for (x,y) representation, x means n_e quantum number of electron and y means n_h quantum number of hole (for example (1,2) means electron is at ground state and hole is at first excited state). All peaks are normalized to 1.

3.3. CdTe-ZnS

In this study, the other structure that is analyzed is (CdTe) ZnS) CdTe) ZnSe). According to our calculation, it is remarkable that for many different core radii with different shell sizes, (CdTe) ZnS) CdTe) ZnSe) structure have multi-color light emission. Consequently, (CdTe) ZnS) CdTe) ZnSe) quantum dot is more efficient than (CdSe) CdS) CdSe) CdS) quantum dot and (CdSe) ZnS) CdSe) ZnS) quantum dot to obtain multi-color emission.

Firstly, in Table 3.4, some specific multi-color emissions are given for 1.29 nm core radius. According to our calculations, when the structure has 3 ML ZnSwith 1 ML CdTe shell, it gives different colors which are orange, green and blue. (1,2),(2,2) and (3,1) are states of electrons and holes, respectively. For 4 ML ZnS shell with 1 ML CdTe shell case gives nearly same colors of emissions and also (1,2), (2,2) which are states of emitting electron and hole couple are same with 3 ML ZnS with 1 ML CdTe shell case. For 3 ML ZnS shell with 2 ML CdTe shell, quantum dot have almost same colors of emissions with 4 ML ZnS shell with 2 ML CdTe shell but emissions are from

Table 3.3. Some specific multi-color emission results for the structure (CdSe) CdS) CdSe) CdS) when core radius is **2.02** and **2.52** nm

Core Radius (nm)	**Shell Size (ML)**	**Shell Size (ML)**	**States ($\mathbf{n}_e, \mathbf{n}_h$)**	**Transition Energy (eV)**	**Oscillator Strength**
2.02	2	4	(2,3)	2.02	4
			(2,2)	2.88	3
2.02	4	4	(2,3)	2.26	3
			(2,1)	2.06	2
2.52	4	1	(2,2)	1.81	7
			(3,2)	1.95	5
			(1,2)	2.04	3
2.52	4	4	(2,2)	1.86	8
			(3,3)	2.17	5

Table 3.4. Some specific multi-color emission results for the structure (CdTe) ZnS) CdTe) ZnS) when core radius is **1.29** nm

Core Radius (nm)	**Shell Size (ML)**	**Shell Size (ML)**	**States ($\mathbf{n}_e, \mathbf{n}_h$)**	**Transition Energy (eV)**	**Oscillator Strength**
1.29	3	1	(1,2)	2.02	5
			(2,2)	2.36	4
			(3,2)	2.67	3
1.29	3	2	(2,1)	2.59	1
			(2,2)	3.02	1
1.29	4	1	(1,2)	2.10	1
			(2,2)	2.40	1
1.29	4	2	(2,1)	2.63	5
			(2,3)	3.06	4

different states of electron-hole couples. Thus, for (CdSe) ZnS) CdSe) ZnS) nanocrystal, it is possible to say that when nanocrystal have 1.29 nm radius with 3 or 4 ML ZnS shell, colors of emissions are determined by thickness CdTe shell (second shell).

In edition to this, in Table 3.5, it is given that for structure having 1.93 nm core, despite varying the ZnS shell from 2 ML to 4 ML, emission energies do not change also the states of electron hole pairs are same if CdTe shell is 3 ML. So CdTe shell thickness determines multi-emission colors.

According to our calculations, some other multi-color emissions are obtained from the structure (CdTe) ZnS) CdTe) ZnS) when the core sizes are 2.58 nm and 3.23 nm. In Table 3.6, first 4 rows list the results for 2.58 nm core radius. It is shown that 3 ML ZnS shell with 1 ML CdTe shell and 4 ML ZnS shell with 1 ML CdTe shell structures have

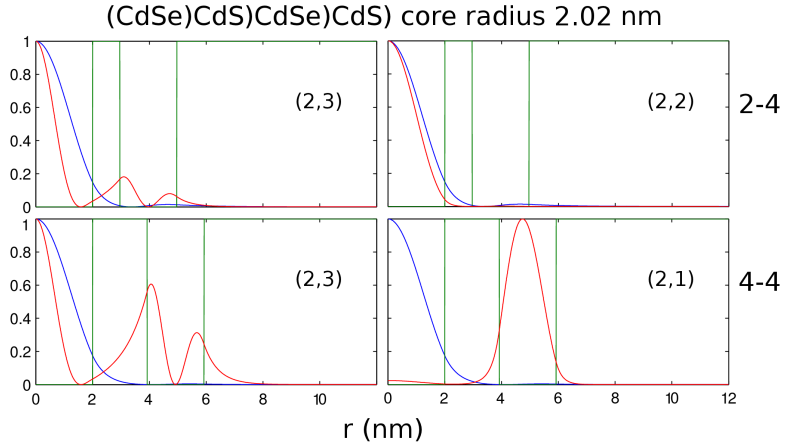

Figure 3.3. Relative probability distribution of electron (blue) $|R_e(r_e)|^2$, hole (red) $|R_h(r_h)|^2$ and potential(green) $V(r)$ of structure (CdSe)CdS)CdSe)CdS) with core radius 2.02 nm. In our notation, x-y means x mono-layer first shell and y mono-layer second shell (for example '2-4' indicates 2 mono-layer first shell and 4 mono-layer second shell). Also for (x,y) representation, x means n_e quantum number of electron and y means n_h quantum number of hole (for example (2,3) means electron is at first excited state and hole is at second excited state). All peaks are normalized to 1.

almost same emission energies. Those emissions are from the same states of which are (1,3) and (2,3). In Figure 3.5, it is shown that, for both pair of states ((1,3),(2,3)), electrons are localized at CdTe core and holes are localized at CdTe shell. Emission energies from the state (1,3) are exactly the same but for 4 ML ZnS shell, emission energy from the state (2,3) is a little bit larger than for 3 ML ZnS shell because of stronger barrier.

Similar relation ship between the structures which have 3 ML ZnS shell with 4 ML CdTe shell and 4 ML ZnS shell with 4 ML CdTe shell. For both structures, energies of emissions and also the states of those emissions are the same. And electrons of emitting

Table 3.5. Some specific multi-color emission results for the structure (CdTe) ZnS) CdTe) ZnS) when core radius is **1.93** nm

Core Radius (nm)	**Shell Size (ML)**	**Shell Size (ML)**	**States (n_e, n_h)**	**Transition Energy (eV)**	**Oscillator Strength**
1.93	2	3	(2,1) (3,3)	2.18 2.63	3 2
1.93	3	3	(2,1) (3,3)	2.23 2.60	7 5
1.93	4	3	(1,2) (3,3)	2.23 2.59	8 7

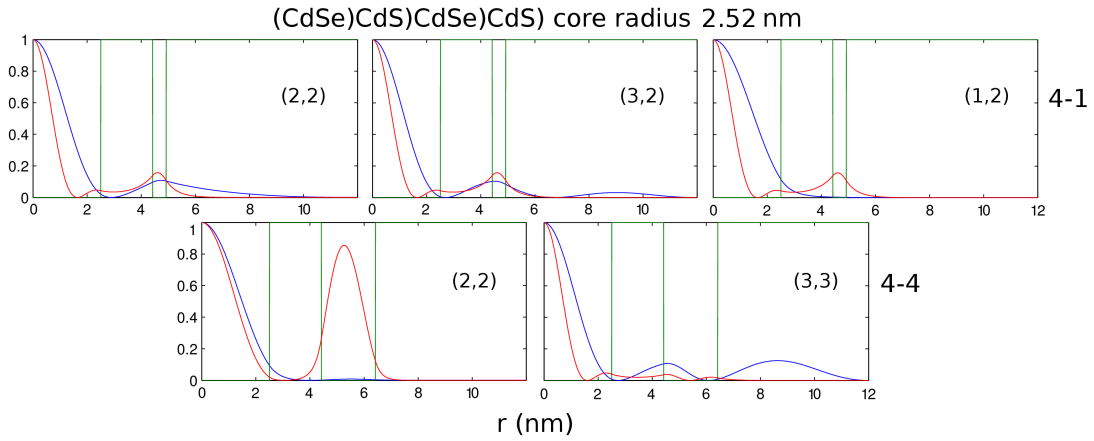

Figure 3.4. Relative probability distribution of electron (blue) $|R_e(r_e)|^2$, hole (red) $|R_h(r_h)|^2$ and potential(green) $V(r)$ of structure (CdSe) CdS) CdSe) CdS) with core radius 2.52 nm. In our notation, x-y means x mono-layer first shell and y mono-layer second shell (for example '4-1' indicates 4 mono-layer first shell and 1 monolayer second shell). Also for (x,y) representation, x means n_e quantum number of electron and y means n_h quantum number of hole (for example (2,2) means electron and hole are at first excited state). All peaks are normalized to 1.

states are localized at CdTe core and holes are localized at 4 ML CdTe shell which is shown in Figure 3.5..

For 2.58 nm core radius, multi color emission is determined by the CdTe shell thickness which means that increasing the ZnS shell thickness from 3 ML to 4 ML does not change the multi color emission energies as it is observed and reported in this study for smaller core radii.

Remarkable results are obtained from the structure with 3.23 nm core. In Table 3.6, last 4 row list the results of multi color emitting cases which have 3.23 nm CdTe core, ZnS shell with thickness from 1 ML to 4 ML and CdTe shell with thickness 1 ML. The structures with 1 ML and 2 ML ZnS shell, have the same emitting states which are (2,3) and (3,3). Those states have different emission energies but for both, electrons and holes are localized at CdTe core. On the other hand, the structures with 3 ML and 4 ML ZnS shell, have three different color of emissions. Both have nearly the same energies and the same states of electrons and holes have emissions. One of those emission energies is at range of color green, the other one is at the range of blue, and the last one, which have smallest oscillator strength, isn at the range of red. So these combination of color is very close to white light which is the real achievement. In addition to this, the structures with 3 ML and 4 ML ZnS shell have same CdTe shell with 1 ML thickness. Thus, it is possible to say that also for those structures, CdTe shell determines the emission as all

Table 3.6. Some specific multi-color emission results for the structure (CdTe) ZnS) CdTe) ZnS) when core radius is **2.58** and **3.23** nm

Core Radius (nm)	**Shell Size (ML)**	**Shell Size (ML)**	**States ($\mathbf{n}_e, \mathbf{n}_h$)**	**Transition Energy (eV)**	**Oscillator Strength**
2.58	3	1	(2,3)	1.77	2
			(1,3)	2.26	1
2.58	3	4	(3,3)	2.17	1
			(2,1)	1.96	1
2.58	4	1	(1,3)	2.26	3
			(2,3)	1.88	2
2.58	4	4	(3,3)	2.22	3
			(2,1)	1.96	2
3.23	1	1	(2,3)	1.91	4
			(3,2)	2.38	3
3.23	2	1	(2,3)	2.16	3
			(3,2)	1.66	2
3.23	3	1	(2,3)	2.29	4
			(3,3)	2.62	3
			(2,2)	1.68	2
3.23	4	1	(2,3)	2.31	9
			(3,3)	2.67	8
			(2,2)	1.83	4

(CdTe) ZnS) CdTe) ZnS) multi-color emitting structures.

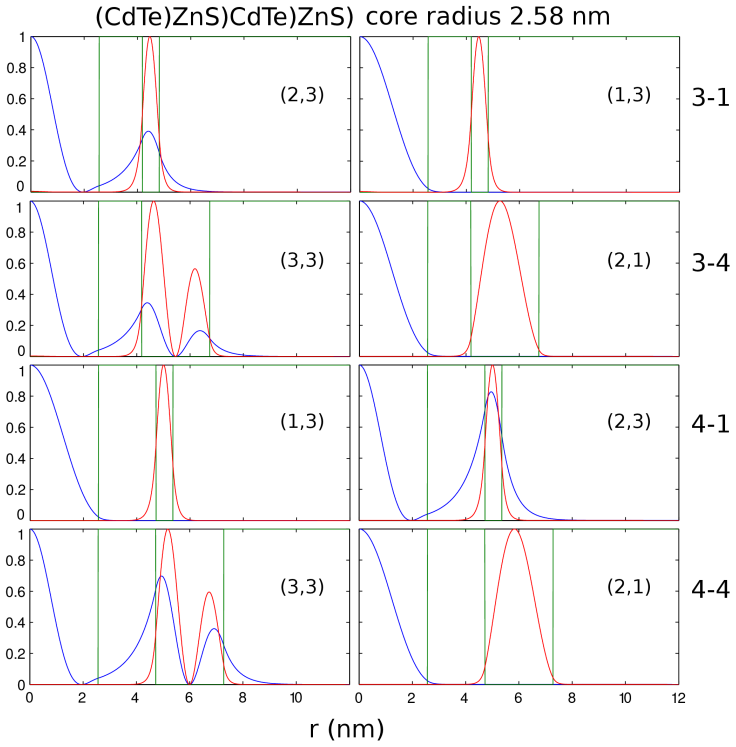

Figure 3.5. Relative probability distribution of electron (blue) $|R_e(r_e)|^2$, hole (red) $|R_h(r_h)|^2$ and potential(green) $V(r)$ of structure (CdTe) ZnS) CdTe) ZnS) with core radius 2.58 nm. In our notation, x-y means x mono-layer first shell and y mono-layer second shell (for example '3-1' indicates 3 mono-layer first shell and 1 mono-layer second shell). Also for (x,y) representation, x means n_e quantum number of electron and y means n_h quantum number of hole (for example (2,3) means electron is at first excited state and hole is at second excited state). All peaks are normalized to 1.

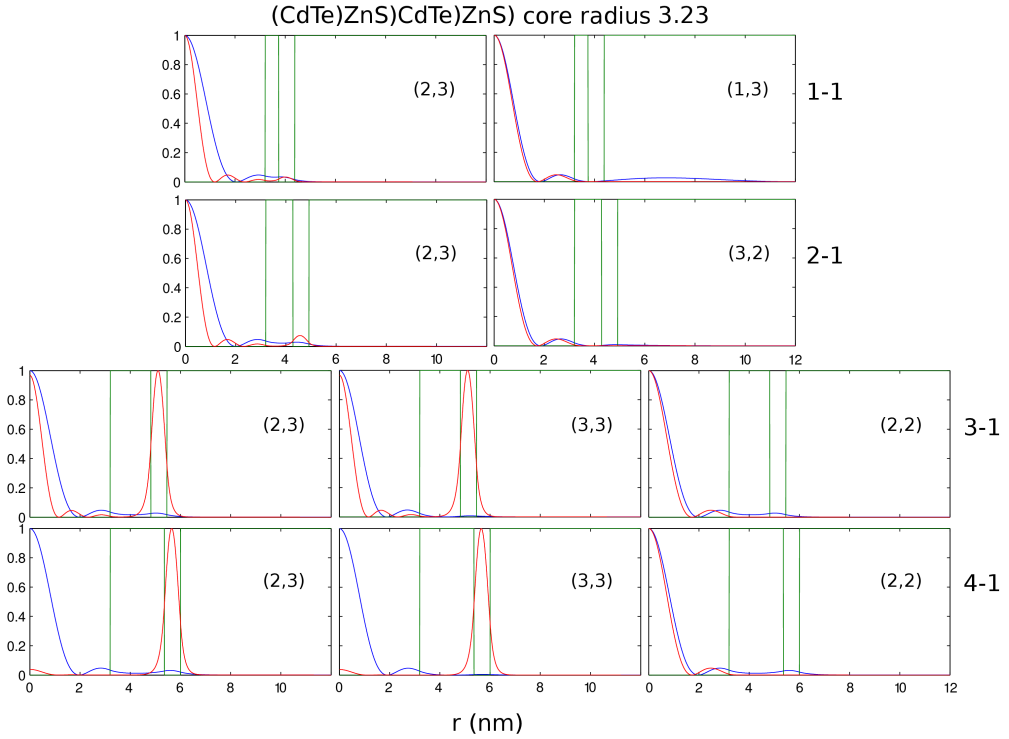

Figure 3.6. Relative probability distribution of electron (blue) $|R_e(r_e)|^2$, hole (red) $|R_h(r_h)|^2$ and potential(green) $V(r)$ of structure (CdTe) ZnS) CdTe) ZnS) with core radius 3.23 nm. In our notation, x-y means x mono-layer first shell and y mono-layer second shell (for example '1-1' indicates 1 mono-layer first shell and 1 mono-layer second shell). Also for (x,y) representation, x means n_e quantum number of electron and y means n_h quantum number of hole (for example (2,3) means electron is at first excited state and hole is at second excited state). All peaks are normalized to 1.

CHAPTER 4

CONCLUSION

Localizations of electron and hole, and the resulting excitonic light emission are calculated in multishell spherical quantum dot structures under several approximations. It is demonstrated that the emitted light color and transition rates can be engineered by changing core size shell thicknesses, and material combinations. We showed that in some specific quantum dots multi color emission can be obtained.

Three different pairs of semiconductors are considered in this study. One of them is (CdSe) ZnS) CdSe) ZnSe), other is (CdSe) CdS) CdSe) CdSe) and third one is (CdTe) ZnS) CdTe) ZnSe). According to our calculation, (CdSe)ZnS)CdSe)ZnSe) structure, when the core radius is 1.51 nm with some different shells combinations, has multi-color emissions from higher frequency to lower frequency in the visible spectrum. (CdSe) CdS) CdSe) CdSe) structure has multi-color emissions when the core radii are 2.02 nm and 2.52 nm yet this structure is the most inefficient structures which we analyse. Moreover, multi-color emissions are obtained from the structure (CdTe) ZnS) CdTe) ZnS) when the core radii are 1.29 nm, 1.93 nm, 2.58 nm and 3.23 nm. Also, this structure has nearly white light emission for 3.23 nm core radius with 3 ML ZnS shell and 1 ML CdTe shell, and with 4 ML ZnS shelland 1 ML CdTe shell.

REFERENCES

[1] S. Nizamoglu and H.V. Demir. Onion-like (cdse) zns/cdse/zns quantum-dot-quantum-well heteronanocrystals for investigation of multi-color emission. *Optics express*, 16(6):3515–3526, 2008.

[2] O. Madelung. *Semiconductors: data handbook*. Springer Verlag, 2004.

[3] C.R. Berry. Effects of Crystal Surface on the Optical Absorption Edge of AgBr. *Physical Review*, 153(3):989, 1967.

[4] C.R. Berry. Structure and optical absorption of AgI microcrystals. *Physical Review*, 161(3):848, 1967.

[5] E.J. Meehan and J.K. Miller. Complex refractive index of colloidal silver bromide in the near-ultraviolet. *The Journal of Physical Chemistry*, 72(5):1523–1529, 1968.

[6] J.R. Arthur. Interaction of Ga and As2 molecular beams with GaAs surfaces. *Journal of Applied Physics*, 39(8):4032–4034, 1968.

[7] A.Y. Cho. Film deposition by molecular-beam techniques. *Journal of Vacuum Science & Technology*, 8(5):S31–&, 1971. K2803 Times Cited:109 Cited References Count:29.

[8] R. Dingle, W. Wiegmann, and C.H. Henry. Quantum States of Confined Carriers in Very Thin AlxGa1- x As-GaAs–AlxGa1- x As Heterostructures. *Phys. Rev. Lett*, 33(14):827–830, 1974.

[9] L.E. Brus. Electron electron and electron-hole interactions in small semiconductor crystallites - the size dependence of the lowest excited electronic state. *Journal of Chemical Physics*, 80(9):4403–4409, 1984. Sq656 Times Cited:2129 Cited References Count:20.

[10] A.L. Efros and A.L. Efros. Interband light absorption in semiconductor sphere. *Semiconductors*, 16:1209–1214, 1982.

[11] A.I. Ekimov and A.A. Onushchenko. Size quantization of the electron energy spectrum in a microscopic semiconductor crystal. *JETP Lett*, 40(8):1136–1139, 1984.

[12] H. Weller, H.M. Schmidt, U. Koch, A. Fojtik, S. Baral, A. Henglein, W. Kunath, K. Weiss, and E. Dieman. Photochemistry of colloidal semiconductors. onset of light absorption as a function of size of extremely small cds particles. *Chemical physics letters*, 124(6):557–560, 1986.

[13] Y. Kayanuma. Wannier exciton in microcrystals. *Solid state communications*, 59(6):405–408, 1986.

[14] H.M. Schmidt and H. Weller. Quantum size effects in semiconductor crystallites: calculation of the energy spectrum for the confined exciton. *Chemical physics letters*, 129(6):615–618, 1986.

[15] M.G. Bawendi, M.L. Steigerwald, and L.E. Brus. The quantum mechanics of larger semiconductor clusters (" quantum dots"). *Annual Review of Physical Chemistry*, 41(1):477–496, 1990.

[16] L. Banyai, Y.Z. Hu, M. Lindberg, and S.W. Koch. Third-order optical nonlinearities in semiconductor microstructures. *Physical Review B*, 38(12):8142, 1988.

[17] S. Schmitt-Rink, D.A.B. Miller, and D.S. Chemla. Theory of the linear and nonlinear optical properties of semiconductor microcrystallites. *Physical Review B*, 35(15):8113, 1987.

[18] Y.Z. Hu, M. Lindberg, and S.W. Koch. Theory of optically excited intrinsic semiconductor quantum dots. *Physical Review B*, 42(3):1713, 1990.

[19] Y.Z. Hu, SW Koch, M. Lindberg, N. Peyghambarian, EL Pollock, and F.F. Abraham. Biexcitons in semiconductor quantum dots. *Physical review letters*, 64(15):1805–1807, 1990.

[20] J.J. Ramsden and M. Gr
"atzel. Photoluminescence of small cadmium sulphide particles. *J. Chem. Soc., Faraday Trans. 1*, 80(4):919–933, 1984.

[21] S.H. Park, R.A. Morgan, Y.Z. Hu, M. Lindberg, S.W. Koch, and N. Peyghambarian. Nonlinear optical properties of quantum-confined cdse microcrystallites. *JOSA B*, 7(10):2097–2105, 1990.

[22] Y. Wang, N. Herron, W. Mahler, and A. Suna. Linear-and nonlinear-optical properties of semiconductor clusters. *JOSA B*, 6(4):808–813, 1989.

[23] L. Spanhel, M. Haase, H. Weller, and A. Henglein. Photochemistry of colloidal semiconductors. 20. surface modification and stability of strong luminescing cds particles. *Journal of the American Chemical Society*, 109(19):5649–5655, 1987.

[24] H. Weller, U. Koch, M. Gutierrez, and A. Henglein. Photochemistry of colloidal metal sulfides .7. absorption and fluorescence of extremely small zns particles - the world of the neglected dimensions. *Berichte Der Bunsen-Gesellschaft-Physical Chemistry Chemical Physics*, 88(7):649–656, 1984. Te197 Times Cited:205 Cited References Count:16.

[25] H. Youn, S. Baral, and J.H. Fendler. Dihexadecyl phosphate, vesicle-stabilized and in situ generated mixed cds and zns semiconductor particles. preparation and utilization for photosensitized charge separation and hydrogen generation. *J. Phys. Chem.;(United States)*, 92(22), 1988.

[26] A. Henglein, M. Gutierrez, K. Weller, A. Fojtik, and J. Jirkovskỳ. Photochemistry of colloidal semiconductors 30. reactions and fluorescence of agi and agi agi2s colloids. *Berichte der Bunsengesellschaft f
”ur physikalische Chemie*, 93(5):593–600, 1989.

[27] A.R. Kortan, R. Hull, R.L. Opila, M.G. Bawendi, M.L. Steigerwald, PJ Carroll, and L.E. Brus. Nucleation and growth of cadmium selendie on zinc sulfide quantum crystallite seeds, and vice versa, in inverse micelle media. *Journal of the American Chemical Society*, 112(4):1327–1332, 1990.

[28] C.F. Hoener, K.A. Allan, A.J. Bard, A. Campion, M.A. Fox, and T.E. Mallouk. Webber se and white jm. *J. Phys. Chem.*, 1992:96, 1992.

[29] H.S. Zhou, I. Honma, H. Komiyama, and J.W. Haus. Coated semiconductor nanoparti-

cles; the cadmium sulfide/lead sulfide system's synthesis and properties. *The Journal of Physical Chemistry*, 97(4):895–901, 1993.

[30] A. Hasselbarth, A. Eychmuller, R. Eichberger, M. Giersig, A. Mews, and H. Weller. Chemistry and photophysics of mixed cds/hgs colloids. *Journal of Physical Chemistry*, 97(20):5333–5340, 1993. Ld042 Times Cited:129 Cited References Count:51.

[31] A. Eychmuller, A. Mews, and H. Weller. A quantum-dot quantum-well - cds/hgs/cds. *Chemical Physics Letters*, 208(1-2):59–62, 1993. Lf013 Times Cited:129 Cited References Count:30.

[32] S.A. Ivanov, J. Nanda, A. Piryatinski, M. Achermann, L.P. Balet, I.V. Bezel, P.O. Anikeeva, S. Tretiak, and V.I. Klimov. Light amplification using inverted core/shell nanocrystals: Towards lasing in the single-exciton regime. *The Journal of Physical Chemistry B*, 108(30):10625–10630, 2004.

[33] R.B. Little, M.A. El-Sayed, G.W. Bryant, and S. Burke. Formation of quantum-dot quantum-well heteronanostructures with large lattice mismatch: Zns/cds/zns. *The Journal of Chemical Physics*, 114:1813, 2001.

[34] D. Battaglia, J.J. Li, Y. Wang, and X. Peng. Colloidal two-dimensional systems: Cdse quantum shells and wells. *Angewandte Chemie International Edition*, 42(41):5035–5039, 2003.

[35] J. Schrier and L.W. Wang. Electronic structure of nanocrystal quantum-dot quantum wells. *Physical Review B*, 73(24):245332, 2006.

[36] X. Zhong, R. Xie, Y. Zhang, T. Basché, and W. Knoll. High-quality violet-to red-emitting znse/cdse core/shell nanocrystals. *Chemistry of materials*, 17(16):4038–4042, 2005.

[37] D. Battaglia, B. Blackman, and X. Peng. Coupled and decoupled dual quantum systems in one semiconductor nanocrystal. *Journal of the American Chemical Society*, 127(31):10889–10897, 2005.

[38] S. Sapra, S. Mayilo, T.A. Klar, A.L. Rogach, and J. Feldmann. Bright white-light emis-

sion from semiconductor nanocrystals: by chance and by design. *Advanced Materials*, 19(4):569–+, 2007. 140ON Times Cited:37 Cited References Count:14.

[39] M.G. Burt. The justification for applying the effective-mass approximation to microstructures. *Journal of Physics-Condensed Matter*, 4(32):6651–6690, 1992. Jj062 Times Cited:300 Cited References Count:51.

[40] L.P. Balet, S.A. Ivanov, A. Piryatinski, M. Achermann, and V.I. Klimov. Inverted core/shell nanocrystals continuously tunable between type-i and type-ii localization regimes. *Nano Letters*, 4(8):1485–1488, 2004. 846CQ Times Cited:58 Cited References Count:11.

[41] D. Dorfs, H. Henschel, J. Kolny, and A. Eychm
”uller. Multilayered nanoheterostructures: Theory and experiment. *The Journal of Physical Chemistry B*, 108(5):1578–1583, 2004.

[42] V.I. Klimov, S.A. Ivanov, J. Nanda, M. Achermann, I. Bezel, J.A. McGuire, and A. Piryatinski. Single-exciton optical gain in semiconductor nanocrystals. *NATURE-LONDON-*, 447(7143):441, 2007.

[43] J.W. Haus, H.S. Zhou, I. Honma, and H. Komiyama. Quantum confinement in semiconductor heterostructure nanometer-size particles. *Physical Review B*, 47(3):1359, 1993.

[44] L.E. Brus. A simple model for the ionization potential, electron affinity, and aqueous redox potentials of small semiconductor crystallites. *The Journal of chemical physics*, 79:5566, 1983.

[45] D.J. BenDaniel and C.B. Duke. Space-charge effects on electron tunneling. *Phys. Rev.*, 152(2):683–692, Dec 1966.

[46] R.T. Senger and K.K. Bajaj. Optical properties of confined polaronic excitons in spherical ionic quantum dots. *Physical Review B*, 68(4):045313, 2003.